Technology in Cancer Research and Treatment
ISSN 1533-0346
Volume 14 Number 4 August 2015
2014 April 16. Epub ahead of print.

Non Tumor Perfusion Changes Following Stereotactic Radiosurgery to Brain Metastases

Raphael Jakubovic, M.Sc.[1,2]
Arjun Sahgal, M.D.[3]
Mark Ruschin, Ph.D.[3]
Ana Pejović-Milić, Ph.D.[2]
Rachael Milwid, B.Sc.[1]
Richard I. Aviv, MRCP, FRCR, FRCPC[1]*

[1]Department of Medical Imaging, Division of Neuroradiology, Sunnybrook Health Sciences Centre, University of Toronto, Toronto, Ontario, Canada
[2]Department of Biomedical Physics, Ryerson University, Toronto, Ontario, Canada
[3]Department of Radiation Oncology, Odette Cancer Centre of the Sunnybrook Health Sciences Centre, University of Toronto, Toronto, Ontario, Canada

www.tcrt.org
DOI: 10.7785/tcrtexpress.2013.600279

Purpose: To evaluate early perfusion changes in normal tissue following stereotactic radiosurgery (SRS). **Methods**: Nineteen patients harboring twenty-two brain metastases treated with SRS were imaged with dynamic susceptibility magnetic resonance imaging (DSC MRI) at baseline, 1 week and 1 month post SRS. Relative cerebral blood volume and flow (rCBV and rCBF) ratios were evaluated outside of tumor within a combined region of interest (ROI) and separately within gray matter (GM) and white matter (WM) ROIs. Three-dimensional dose distribution from each SRS plan was divided into six regions: (1) <2 Gy; (2) 2-5 Gy; (3) 5-10 Gy; (4) 10-12 Gy; (5) 12-16 Gy; and (6) >16 Gy. rCBV and rCBF ratio differences between baseline, 1 week and 1 month were compared. Best linear fit plots quantified normal tissue dose-dependency. **Results**: Significant rCBV ratio increases were present between baseline and 1 month for all ROIs and dose ranges except for WM ROI receiving <2 Gy. rCBV ratio for all ROIs was maximally increased from baseline to 1 month with the greatest changes occurring within the 5-10 Gy dose range (53.1%). rCBF ratio was maximally increased from baseline to 1 month for all ROIs within the 5-10 Gy dose range (33.9-45.0%). Both rCBV and rCBF ratios were most elevated within GM ROIs. A weak, positive but not significant association between dose, rCBV and rCBF ratio was demonstrated. Progressive rCBV and rCBF ratio increased with dose up to 10 Gy at 1 month. **Conclusion**: Normal tissue response following SRS can be characterized by dose, tissue, and time specific increases in rCBV and rCBF ratio.

Key words: Brain; Cancer; Dynamic susceptibility; Imaging; Metastases; MR perfusion; Normal tissue response.

Introduction

SRS is commonly used to treat cerebral metastases. SRS is the delivery of a single high total dose of radiation to a target localized in three dimensions with milli metre precision. SRS has the benefit of increasing tumor control compared to WBRT, but at the expense of a greater risk of radiation-induced necrosis (1).

Abbreviations: CBF: Cerebral Blood Flow; CBV: Cerebral Blood Volume; CSF: Cerebrospinal Fluid; CT: Computed Tomography; DSC: Dynamic Susceptibility Contrast; DWI: Diffusion Weighted Image; ECOG: Eastern Cooperative Oncology Group; FLAIR: Fluid Attenuated Inversion Recovery; FOV: Field of View; FSPGRE: Fast Spoiled Gradient Echo; GM: Gray Matter; KPS: Karnofsky Performance Status; MRI: Magnetic Resonance Imaging; NEX: Number of Excitations; PET: Positron Emission Tomography; rCBV: Relative Cerebral Blood Volume; rCBF: Relative Cerebral Blood Flow; ROI: Region of Interest; RPA: Recursive Partitioning Analysis; RTOG: Radiation Treatment Oncology Group; SD: Standard Deviation; SPGRE: Spoiled Gradient Echo; SPM: Statistical Parametric Mapping; SRS: Stereotactic Radiosurgery; SVD: Singular Value Decomposition; TE: Echo Time; TI: Inversion Time; TR: Repetition Time; WBRT: Whole Brain Radiation Therapy; WM: White Matter.

*Corresponding author:
Richard I. Aviv, MRCP, FRCR, FRCPC
Phone: 416-480-6100; Ext. 7989
E-mail: richard.aviv@sunnybrook.ca

Side effects include acute headaches, nausea, and drowsiness, subacute neurological deterioration and late development of necrosis, worsening neurological status, seizures, and increased intracranial pressure (2, 3). Predictive factors of necrosis have indicated that the dose delivered to normal brain tissue surrounding the targeted tumor is critical [for example, the volume exposed to 10 Gy (V10) or 12 Gy (V12)] (1).

The physiological response of normal tissue to radiation, considered a surrogate of cellular response and dose tolerance, has been shown to differ based on whether there is a single high dose exposure or multiple sessions delivering as fractionated doses (4, 5). SRS mitigates the extent of normal tissue damage by delivering an ablative dose to the tumor coupled with rapid dose fall-off. The efficacy of SRS for metastases is well documented with reported local control $>80\%$ in over 2000 treated patients (6). Perfusion imaging is widely used as a surrogate of tumor response in primary and secondary tumors (7-11). Few studies have evaluated perfusion response within normal tissues following radiotherapy (12-16). A better understanding of the radiobiological effects of SRS, specifically in normal brain tissue would provide insight into tissue specific dose tolerances and potentially guide isodose prescription. Our aim was to determine the physiologic changes within the surrounding normal brain tissue following exposure to SRS using DSC MRI perfusion derived parameters.

Methods

Study Design and Patient Cohort

Nineteen patients treated with SRS were enrolled between March 2008 and April 2011 on an Institutional Research Ethics Board (IRB) approved protocol. Inclusion criteria included brain metastases treated with SRS, age ≥ 18, able to provide consent for the MRI protocol, diagnosis of brain metastases, expected life expectancy greater than 6 months, and KPS greater than 70. Patients with MRI contraindications, prior allergic reaction to gadolinium, or a treatment plan including WBRT were excluded. Baseline clinical parameters recorded included age, gender, tumor volume, radiation dose, steroid administration, RPA score, KPS, and ECOG performance status. Steroid dose was kept constant for 1 week post-treatment and tapered thereafter according to clinical indications to control for possible confounding effects (17).

Imaging Acquisition

DSC MRI was performed at baseline, one week and one month following treatment. Structural MRIs were performed every two months thereafter. MRI brain sequences were performed on a 1.5 T GE Twinspeed (General Electric, Mississauga, Canada) and included a DWI (7000 ms/min [TR/TE], FOV of 24 cm, matrix 128×128, section thickness of 5 mm with no gap); a FLAIR image (8000/120/200 [TR/TE/TI], FOV 24 cm, matrix 320×224, ST 5, 1 mm gap); a sagittal T1 FLAIR image (2200/24/750 [TR/TE/TI], FOV 24 cm, matrix 224×320, NEX 2, ST 5 mm, 1 mm spacing); a 3D T1 SPGRE (8.5/4.2, FA 20, FOV 22 cm, matrix 270×270, NEX 2) and a DSC study (1700/31.5/90, FOV 24 cm; section thickness 5 mm; matrix 128×128; no gap). Gadovist 0.1 mL/kg, 1 mmol/l concentration was injected at 5 mL/s for the DSC study. The DSC study was followed by a post-gadolinium 3D T1FSPGRE with similar parameters to pre-gadolinium sequence.

Radiation Treatment

All patients were treated with SRS alone. The T1 MR images were fused to the stereotactically localized CT images for planning (slice thickness: 1.5 mm, pixel size 0.7 mm). CT-MR fusion was done using an automated rigid image-matching algorithm based on mutual information and was assessed and approved by an experienced radiation oncologist prior to treatment. Treatment planning was performed using the Radionics planning software (Integra Radionics, Burlington, Massachusetts, United States) with radiation doses ranging from 16 Gy to 24 Gy in a single fraction. SRS dose selection was based according to tumor diameter in accordance to RTOG 9005 (18). Dose was prescribed to periphery of the gross tumor volume as delineated on T1-weighted MR images. No planning target volume margin was added. Prescription dose was prescribed to the $90 \pm 5\%$ isodose line. One patient with multiple isocentres was prescribed to the 70% isodose line.

Localization and immobilization was performed using the Brown-roberts-wells head frame. Treatment delivery was performed using 6 MV photons on a Siemens PRIMUS linear accelerator (Siemens AG, Erlangen, Germany), equipped with stereotactic cones ranging from 1.0 cm in diameter up to 4 cm in diameter.

Image Analysis

SRS Dose Distribution Determination: Dose calculation was performed using a pencil-beam based approach based on measured tissue-phantom-ratios, off-axis ratios, and cone output factors. The uncertainty in the measured data was estimated to be on the order of 1%. The cumulative uncertainty in the dose algorithm was difficult to ascertain but the maximum error in calculated dose was within 4-5% for all cone sizes, as validated internally with end-to-end tests and externally via the Radiological Physics Center (MD Anderson, United States).

Pre-treatment SRS localized dose planning CT images with overlaid isodose maps were co-registered to structural 3D T1 SPGRE post-gadolinium images. All co-registrations were performed using a tri-linear interpolation algorithm using SPM12b (Welcome Trust, London, United Kingdom).

MR Images: Tumor volumes were measured using MIPAV (Medical Image Processing, Analysis and Visualization software; Center for Information Technology, National Institutes of Health, version 4.4.1.). A brain tissue probability map template (Montreal Neurological Institute, Montreal, Canada) comprising GM, WM, and CSF was co-registered to the baseline structural T1-post gadolinium images using SPM12b. GM and WM tissue binary masks were generated by applying a 50% threshold to the registered tissue probability maps. DSC maps were calculated with positron emission tomography validated software utilizing SVD (19). Using the central volume principle and an arterial input function CBV and CBF maps were extracted based on susceptibility changes during the passage of contrast through the cerebral tissues. CBV reflects the fraction of tissue volume occupied by blood. CBF reflects the volume of blood traversing a region per unit time (20). DSC maps were co-registered to structural T1-post gadolinium images. Voxels representing cerebral vasculature containing CBV >8 mL/100 g or CBF >100 mL/100 g/min were excluded as previously described (21). A contra-lateral WM mirror region was reflected and used to calculate rCBV and rCBF values.

Dosimetric Analysis: Three-dimensional volume assessments were performed for all marker lesions at all time-points using MIPAV using 3D T1 SPGRE images. Co-registered SRS dose plans were segmented using in-house software developed within MATLAB (MATLAB 2012b, The MathWorks, Inc., Natick, Massachusetts, United States) and superimposed on the rCBV and rCBF maps. The following six irradiated dose levels were defined: <2 Gy and 2-5 Gy (out of target), 5-10 Gy, 10-12 Gy, and 12-16 Gy (peri-target), and >16 Gy (on target). Tumor voxels were removed from analysis. A typical dose distribution is shown in Figure 1. Combined ROIs included both GM and WM. Thresholded tissue probability maps were used to divide combined ROIs further into individual GM and WM ROIs. Percent of total intracranial volume of combined, GM and WM for each dose level were calculated based on intracranial volumes calculated using Individual Brain Atlases using Statistical Parametric Mapping software (IBASPM, Cuban Neuroscience Center, Playa, Ciudad de la Habana, Cuba) (22).

Statistical Analysis

For each SRS dose level and MRI time point, CBF and CBV were extracted from the DSC maps for combined, GM and WM ROIs and expressed as a ratio relative to the contralateral baseline. rCBV and rCBF ratio change between baseline and 1 week and baseline and 1 month for each dose level for combined, GM, and WM were compared using the Wilcoxon signed ranks test. Dose was plotted against rCBV and rCBF ratio for combined, GM, and WM ROIs and a best line linear fit was applied to each set of data. All analyses were performed using SPSS version 21. $P < 0.05$ was considered significant.

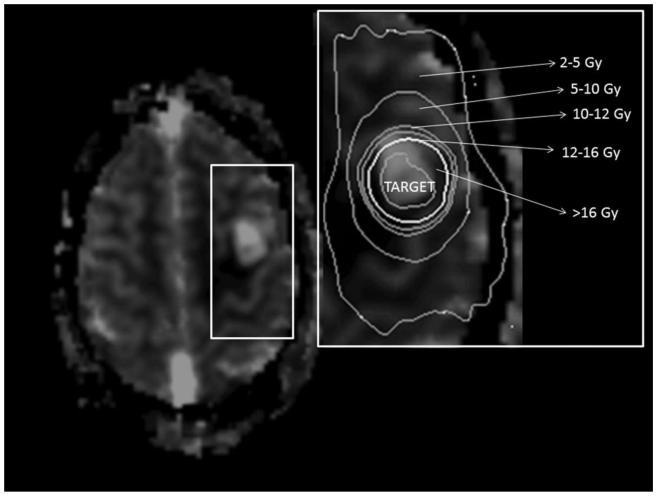

Figure 1: CBV with overlaid dose distribution: 71 year old male patient (KPS 90) diagnosed with brain metastases secondary to colon carcinoma and treated with 18 Gy SRS. Single lesion located in the left precentral gyrus. Target region is drawn for illustrative purposes but was excluded from analysis.

Results

Baseline tumor and patient characteristics for the 19 patients and 22 metastases treated are described in Table I. Median (range) SRS dose was 20 Gy (16-24 Gy) in a single fraction. Mean (SD) intracranial brain volume was 23.52 (3.87) cm^3. The percent of irradiated intracranial volume for each dose level is shown in Table II. rCBV and rCBF ratio stratified by dose for combined, GM and WM ROIs are provided in Table III and Figure 2.

rCBV ratio increased between baseline and 1 week for all ROIs and dose ranges although the increase was not statistically significant. Significant rCBV ratio increase was present between baseline and 1 month for all ROIs and dose ranges with the exception of the WM ROI receiving <2 Gy. rCBV ratio for all ROIs was maximally increased from baseline at 1 month with the greatest changes occurring within the 5-10 Gy dose range. GM ROI rCBV ratio values were most elevated.

rCBF ratio increase occurred within the combined ROI between baseline and 1 week in the >10 Gy dose range. This

Table I
Baseline clinical variables (n = 19 patients, 22 indexed tumors).

Clinical variable	N (%)
Male	10 (52.6)
Previous radiation	9 (47.4)
Previous chemotherapy	15 (78.9)
Recursive partitioning analysis score (RPA)	
1	6 (31.6)
2	1 (5.3)
3	12 (63.1)
Radiation dose (Gy)	Median (range)
	20 (16-24)
Baseline Karnofsky performance status (KPS) median (IQR)	80 (80-90)
Baseline ECOG <2	17 (89.5)
Steroids at baseline	8 (42.1)
Primary tumor diagnosis	
Melanoma	5 (26.3)
Breast	2 (10.5)
Lung	8 (42.1)
Renal cell	3 (15.8)
Colon	1 (5.3)

was driven predominantly by GM changes at the higher dose ranges. rCBF ratio increased between baseline and 1 month for combined ROIs across all dose ranges although the increase was not significant. Significant rCBF ratio increase was, however, present at 1 month for GM dose ranges >10 Gy and WM dose ranges between 5 and 16 Gy. rCBF ratio for all ROIs was maximally increased from baseline at 1 month with the greatest changes occurring within the 5-10 Gy dose range. GM ROI rCBF ratio values were most elevated.

A weak, positive but not significant association between dose, rCBV and rCBF ratio at 1 week and 1 month for all ROIs was demonstrated (Figure 2; rCBV: $\rho = 0.027$-0.114; rCBF: $\rho = 0.042$-0.135). rCBV and rCBF ratio increased progressively with dose between baseline and 1 week driven predominantly by GM changes. WM ROIs increase was also seen but attenuated beyond 10 Gy. At 1 month progressive rCBV and rCBF ratio increase occurred for all ROIs up to 10 Gy.

Table II
Percent of irradiated intracranial volume for each dose level calculated using IBASPM.

%	>16 Gy	12-16 Gy	10–12 Gy	5-10 Gy	2-5 Gy	<2 Gy
Combined	0.094 ± 0.086	0.063 ± 0.045	0.064 ± 0.048	0.525 ± 0.440	2.973 ± 2.264	96.27 ± 2.852
GM	0.141 ± 0.148	0.150 ± 0.128	0.111 ± 0.102	0.786 ± 0.768	3.333 ± 2.284	95.47 ± 3.326
WM	0.039 ± 0.031	0.042 ± 0.029	0.035 ± 0.026	0.330 ± 0.310	1.906 ± 1.566	97.64 ± 1.925

Table III
Mean and standard deviation rCBV and rCBF ratio values at 1 week and 1 month following radiation for combined, GM, and WM ROIs segmented by dose. *P* values were obtained using non-parametric Wilcoxon sum rank univariate analysis.

	>16 Gy	12-16 Gy	10-12 Gy	5-10 Gy	2-5 Gy	<2 Gy
rCBV ratio baseline to 1 week						
Combined	1.279 ± 0.794	1.256 ± 0.733	1.244 ± 0.677	1.191 ± 0.509	1.201 ± 0.470	1.189 ± 0.471
GM	1.307 ± 0.657	1.230 ± 0.606	1.231 ± 0.609	1.168 ± 0.502	1.174 ± 0.458	1.171 ± 0.506
WM	1.134 ± 0.304	1.112 ± 0.282	1.108 ± 0.258	1.168 ± 0.485	1.120 ± 0.364	1.125 ± 0.394
rCBV ratio baseline to 1 month						
Combined	1.374 ± 0.661*	1.382 ± 0.606*	1.417 ± 0.643*	1.422 ± 0.666*	1.362 ± 0.661*	1.274 ± 0.477*
GM	1.404 ± 0.565*	1.449 ± 0.640*	1.499 ± 0.678*	1.531 ± 0.820*	1.467 ± 0.911*	1.258 ± 0.470*
WM	1.166 ± 0.194*	1.253 ± 0.309*	1.289 ± 0.379*	1.379 ± 0.568*	1.297 ± 0.532*	1.258 ± 0.501
rCBF ratio baseline to 1 week						
Combined	1.253 ± 0.522*	1.229 ± 0.473*	1.205 ± 0.441*	1.183 ± 0.396	1.155 ± 0.375	1.127 ± 0.333
GM	1.254 ± 0.444*	1.219 ± 0.414*	1.203 ± 0.437	1.160 ± 0.399	1.126 ± 0.385	1.127 ± 0.392
WM	1.175 ± 0.331	1.173 ± 0.321	1.175 ± 0.358	1.199 ± 0.415	1.123 ± 0.321	1.108 ± 0.286
rCBF ratio baseline to 1 month						
Combined	1.314 ± 0.507	1.321 ± 0.501	1.317 ± 0.508	1.339 ± 0.553	1.278 ± 0.564	1.166 ± 0.363
GM	1.369 ± 0.507*	1.436 ± 0.610*	1.436 ± 0.620*	1.450 ± 0.684	1.371 ± 0.786	1.178 ± 0.364
WM	1.247 ± 0.402	1.324 ± 0.415*	1.343 ± 0.440*	1.379 ± 0.501*	1.288 ± 0.488	1.223 ± 0.424

P values less than 0.05 are denoted by an asterisk.

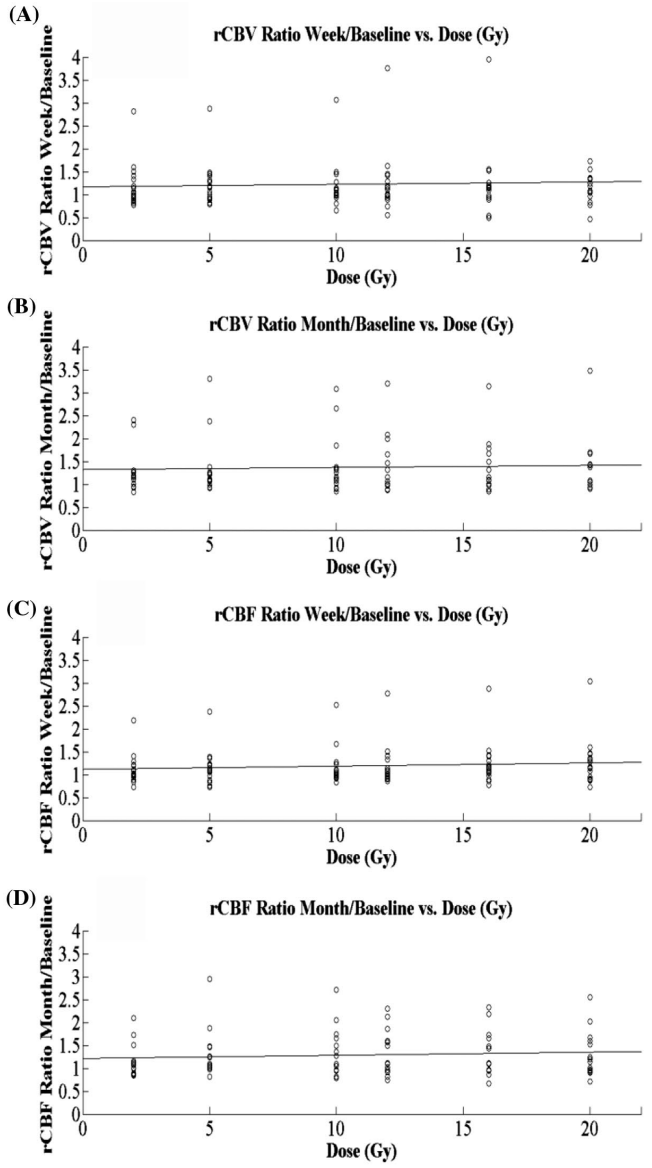

Figure 2: Line of best fit for combined rCBV and rCBF ratio. (**A, B**) rCBV and (**C, D**) rCBF ratio Week/Baseline and Month/Baseline. A weak positive correlation for all tissue types for dose and perfusion was demonstrated.

Discussion

We demonstrate rCBV and rCBF ratios increasing in the adjacent normal brain tissues following SRS to brain metastases. These increases relative to baseline were maximal at 1 month and within the 5-10 Gy dose range (rCBV: 42.2%; rCBF: 33.9%). Progressive increases with dose were present, although the correlation was weakly positive due to a ceiling effect observed at 10 Gy. The highest rCBV and rCBF ratio increase was present in GM ROIs (rCBV: 25.8-53.1%; rCBF: 17.8-45.0%) with sparing of WM in the <2 Gy dose range.

The results of our study indicate that early SRS tissue response within normal tissues occurs in a dose, tissue, and time specific manner. rCBV and rCBF ratios could be surrogates of endothelial apoptosis, vascular damage and radionecrosis, and may provide a framework for the delineation of GM and WM tissue-specific dose tolerances in normal tissue and the integration of these tolerances into an isodose prescription. Further study with repeated imaging and clinical/radiographic response is required and now underway at our institution.

Our results also highlight the dose-sparing effect of SRS with over 96% of the total intracranial volume receiving <2 Gy of radiation (Table II) with no early WM perfusion changes seen following SRS (Table III) in the low dose region. This is consistent with sparing of a significant volume of normal tissue from SRS related effects. However, increased GM ROI rCBV ratio was present even in the <2 Gy dose range (25.8%) reflecting greater radiation perfusion response of these regions presumably due to higher metabolic demand (12, 13). Supporting these findings, WM ROI rCBV and rCBF increase is previously shown in regions receiving <2 Gy following a single fraction of WBRT (23). Preferential GM ROIs rCBV involvement is also previously shown in a study reporting a reduction at 6 months following fractionated conformal and whole brain radiotherapy (12, 13). The prior findings and present study results are consistent with early acute rCBV and rCBF ratio increases with preferentially GM involvement followed by later reduction. This reduction was not seen in our cohort since follow-up perfusion imaging was not obtained past the one month time-point. The precise biological cause and pathophysiological nature of these GM rCBV ratio changes remains unclear.

The response to SRS of normal tissue is largely unknown and perfusion response is varied (15, 16). We demonstrate an incremental rCBV and rCBF ratio increase with dose up to 10 Gy. Several time and dose dependant biological mechanisms in normal tissues are associated with increasing radiation dose including vessel dilation, endothelial cell death and apoptosis (24). Endothelial apoptosis and subsequent cell death begins within twenty-four hours of irradiation and continues up to 1 month followed by a dose independent decrease in cell density up to 6 months (25, 26).

rCBV and rCBF ratio was maximal at 1 month with a progressive increase with dose and ceiling effect at 10 Gy (Table III). Maximum dose effect was seen between 5 and 10 Gy. Whereas doses of 2-5 Gy and 5-12 Gy have been shown to be effective in direct death of oxygenated and hypoxic cells respectively, doses higher than 10-12 Gy induce indirect cell death via vascular damage (1, 27, 28). A rapid increase in vascular volume and permeability over the course of fractionated partial brain radiotherapy

followed by a rapid drop-off by 1 month after treatment has also been shown to occur in a dose and time dependent fashion resulting in vascular regression (9). This regression is attributed to capillary collapse and/or occlusion caused by endothelial cell death, and is referred to as "vessel renormalization". This suggests that regions with greater vascular damage would exhibit an earlier perfusion response followed by vascular regression in regions receiving >10 Gy by 1 month.

Limitations of this study include the administration of previous radiation and chemotherapy, lack of control for dexamethasone dose beyond the 1 week scan, and heterogeneity of tumor types. Patient life expectancy, particularly in a cohort of metastatic brain lesions further limited our ability to assess the association between normal tissue response and radio-necrosis. Although the patient cohort studied represents the largest perfusion cohort reported to date, statistical power was limited by the number of patients. The magnitude of change for each tissue type was modest and insufficient to discriminate individual dose ranges although a preferential increase in GM was seen.

In conclusion we observed time, dose, and tissue specific increases in rCBV and rCBF ratio within normal tissue driven predominantly by GM change. Sparing of significant volume of WM receiving <2 Gy was identified. Further study is required to investigate whether these biomarkers reflect an increased risk of radionecrosis in normal tissue.

Conflict of Interest Statement

There are no conflicts of interest to report.

References

1. Minniti G, Clarke E, Lanzetta G, Osti MF, Trasimeni G, Bozzao A, Romano A & Enrici RM. Stereotactic radiosurgery for brain metastases: analysis of outcome and risk of brain radionecrosis. *Radiat Oncol 6*(48), 1-9 (2011). DOI: 10.1186/1748-717X-6-48
2. Constine LS, Konski A, Ekholm S, McDonald S & Rubin P. Adverse effects of brain irradiation correlated with MR and CT imaging. *Int J Radiat Oncol Biol Phys 15*, 319-30 (1988). DOI: 10.1016/S0360-3016(98)90011-6
3. Tsuruda JS, Kortman KE, Bradley WG, Wheeler DC, Van Dalsem W & Bradley TP. Radiation effects on cerebral white matter: MR evaluation. *AJR Am J Roentgenol 149*, 165-171 (1987). DOI:10.2214/ajr.149.1.165
4. Wood K, Jawahar A, Smelley C, Mullapudi S, DeLaune A, Nanda A & Granger DN. Exposure of brain to high-dose, focused gamma rays irradiation produces increase in leukocytes-adhesion and pavementing in small intracerebral blood vessels. *Neurosurgery 57*, 1282-1288 (2005). DOI: 10.1227/01.NEU.0000187318.17832.55
5. Burnet NG, Johansen J, Turesson I, Nyman J & Peacock JH. Describing patients' normal tissue reactions: concerning the possibility of individuaising radiotherapy dose prescriptions based on potential predictive assays of normal tissue radiosensitivity. Steering Committee of the BioMed2 European Union. *Int J Cancer 79*, 606-613 (1998). DOI:10.1002/(SICI)1097-0215(19981218)79:6<606::AID-IJC9>3.0.CO;2-Y
6. Loeffler JS, Barker FG & Chapman PH. Role of radiosurgery in the management of central nervous system metastases. *Cancer Chemother Pharmacol 43*, S11-S14 (1999). DOI: 10.1007/s002800051092
7. Essig M, Waschkies M, Wenz F, Debus J, Hentrich HR & Knopp MV. Assessment of brain metastases with dynamic susceptibility-weighted contrast-enhanced MR imaging: initial results. *Radiology 228*, 193-199 (2003). DOI: 10.1148/radiol.2281020298
8. Cao Y, Tsien CI, Nagesh V, Junck L, Ten Haken R, Ross BD, Chenevert TL & Lawrence TS. Survival prediction in high-grade gliomas by MRI perfusion before and during early stage of RT [corrected]. *Int J Radiat Oncol Biol Phys 64*, 876-885 (2006). DOI: 10.1016/j.ijrobp.2005.09.001
9. Cao Y, Tsien CI, Sundgren PC, Nagesh V, Normolle D, Buchtel H, Junck L & Lawrence TS. Dynamic contrast-enhanced magnetic resonance imaging as a biomarker for prediction of radiation-induced neurocognitive dysfunction. *Clin Cancer Res 15*, 1747-1754 (2009). DOI:10.1158/1078-0432.CCR-08-1420
10. Millar B-AM, Purdie TG, Yeung I, Pond GR, Billingsley S, Wong R, Haddad P, Wong CS & Laperriere N. Assessing perfusion changes during whole brain irradiation for patients with cerebral metastases. *J Neurooncol 71*, 281-286 (2005). DOI: 10.1007/s11060-004-1722-2
11. Bulakbasi N, Kocaoglu M, Farzaliyev A, Tayfun C, Ucoz T & Somuncu I. Assessment of diagnostic accuracy of perfusion MR imaging in primary and metastatic solitary malignant brain tumors. *AJNR Am J Neuroradiol 26*, 2187-2199 (2005). PMID: 16219821
12. Wenz F, Rempp K, Hess T, Debus J, Brix G, Engenhart R, Knopp MV, van Kaick G & Wannenmacher M. Effect of radiation on blood volume in low-grade astrocytomas and normal brain tissue: quantification with dynamic susceptibility contrast MR imaging. *AJR Am J Roentgenol 166*, 187-193 (1996). DOI: 10.2214/ajr.166.1.8571873
13. Fuss M, Wenz F, Scholdei R, Essig M, Debus J, Knopp MV & Wannenmacher M. Radiation-induced regional cerebral blood volume (rCBV) changes in normal brain and low-grade astrocytomas: quantification and time and dose-dependent occurrence. *Int J Radiat Oncol Biol Phys 48*, 53-58 (2000). PMID: 10924971
14. Price SJ, Jena R, Burnet NG, Hutchinson PJ, Dean AF, Peña A, Pickard JD, Carpenter TA & Gillard JH. Improved delineation of glioma margins and regions of infiltration with the use of diffusion tensor imaging: an image-guided biopsy study. *AJNR Am J Neuroradiol 27*, 1969-1974 (2006). PMID: 16032877
15. Taki S, Higashi K, Oguchi M, Tamamura H, Tsuji S, Ohta K, Tonami H, Yamamoto I, Okamoto K & Iizuka H. Changes in regional cerebral blood flow in irradiated regions and normal brain after stereotactic radiosurgery. *Ann Nucl Med 16*, 273-277 (2002). DOI: 10.1007/BF03000106
16. Weber M-A, Günther M, Lichy MP, Delorme S, Bongers A, Thilmann C, Essig M, Zuna I, Schad LR, Debus J & Schlemmer HP. Comparison of arterial spin-labeling techniques and dynamic susceptibility-weighted contrast-enhanced MRI in perfusion imaging of normal brain tissue. *Invest Radiol 38*, 712-718 (2003). DOI: 10.1097/01.rli.0000084890.57197.54
17. Ostergaard L, Hochberg FH, Rabinov JD, Sorensen AG, Lev M, Kim L, Weisskoff RM, Gonzalez RG, Gyldensted C & Rosen BR. Early changes measured by magnetic resonance imaging in cerebral blood flow, blood volume, and blood-brain barrier permeability following dexamethasone treatment in patients with brain tumors. *J Neurosurg 90*, 300-305 (1999). DOI: 10.3171/jns.1999.90.2.0300
18. Shaw E, Scott C, Souhami L, Dinapoli R, Kline R, Loeffler J & Farnan N. Single dose radiosurgical treatment of recurrent previously irradiated primary brain tumors and brain metastases: final report

of RTOG protocol 90-05. *Int J Radiat Oncol 47*, 291-298 (2000). DOI: 10.1016/S0360-3016(99)00507-6

19. Kudo K, Terae S, Katoh C, Oka M, Shiga T, Tamaki N & Miyasaka K. Quantitative cerebral blood flow measurement with dynamic perfusion CT using the vascular-pixel elimination method: comparison with H2(15)O positron emission tomography. *AJNR Am J Neuro radiol 24,* 419-426 (2003). PMID: 12637292
20. Weber MA, Zoubaa S, Schlieter M, Jüttler E, Huttner HB, Geletneky K, Ittrich C, Lichy MP, Kroll A, Debus J, Giesel FL, Hartmann M & Essig M. Diagnostic performance of spectroscopic and perfusion MRI for distinction of brain tumors. *Neurology 66*, 1899-1906 (2006). DOI: 10.1212/01.wnl.0000219767.49705.9c
21. Murphy BD, Fox AJ, Lee DH, Sahlas DJ, Black SE, Hogan MJ, Coutts SB, Demchuk AM, Goyal M, Aviv RI, Symons S, Gulka IB, Beletsky V, Pelz D, Hachinski V, Chan R & Lee TY. Identification of penumbra and infarct in acute ischemic stroke using computed tomography perfusion-derived blood flow and blood volume measurements. *Stroke 37*, 1771-1777 (2006). DOI: 10.1161/01.STR.0000227243.96808.53
22. Alemán-Gómez Y, Melie-García L &Valdés-Hernandez P. IBASPM: Toolbox for automatic parcellation of brain structures. *12th Annual Meeting of the Organization for Human Brain Mapping 27*, 1 (2006).
23. Price SJ, Jena R, Green HAL, Kirkby NF, Lynch AG, Coles CE, Pickard JD, Gillard JH & Burnet NG. Early radiotherapy dose response and lack of hypersensitivity effect in normal brain tissue: a sequential dynamic susceptibility imaging study of cerebral perfusion. *Clin Oncol (R Coll Radiol) 19*, 577-587 (2007). DOI: 10.1016/j.clon.2007.04.010
24. Cao Y. The promise of dynamic contrast-enhanced imaging in radiation therapy. *Semin Radiat Oncol 21*, 147-156 (2011). DOI:10.1016/j.semradonc.2010.11.001
25. Ljubimova NV, Levitman MK, Plotnikova ED & Eidus LK. Endo thelial cell population dynamics in rat brain after local irradiation. *Br J Radiol 64*, 934-940 (1991). PMID: 1954536
26. Peña LA, Fuks Z & Kolesnick RN. Radiation-induced apoptosis of endothelial cells in the murine central nervous system: protection by fibroblast growth factor and sphingomyelinase deficiency. *Cancer Res 60*, 321-327 (2000). PMID: 10667583
27. Milano MT, Usuki KY, Walter KA, Clark D & Schell MC. Stereotactic radiosurgery and hypofractionated stereotactic radiotherapy: normal tissue dose constraints of the central nervous system. *Cancer Treat Rev 37*, 567-578 (2011). DOI: 10.1016/j.ctrv.2011.04.004
28. Song CW, Park H, Griffin RJ & Levitt SH. Radiobiology of stereotactic radiosurgery and stereotactic body radiation therapy. In: Levitt SH, Purdy JA, Perez CA & Vijayakumar S (Eds.), Technical basis of radiation therapy, 5th Edition. Springer-Verlag: Berlin, Heidelberg, 51-61 (2012). DOI: 10.1007/174_2011_264

Received: October 9, 2013; Revised: February 13, 2014; Accepted: March 11, 2014